

EFFECT OF SURFACE PREPARATION ON CORROSION RESISTANCE OF NiCr, NiAl AND NiCrAl ALLOYS IN SUPERCRITICAL WATER

Yunfen Qian¹, Xiao Huang¹ and David Guzonas²

¹Dept. of Mechanical Engineering, Carleton University

² Atomic Energy of Canada Limited, Chalk River Laboratories

Abstract

The corrosive effect of supercritical water on a number of potential coating materials was investigated in this study. Various surface preparation methods were used to prepare four Ni-based alloys including Ni20Cr, Ni5Al, Ni50Cr and Ni20Cr5Al. The surface preparation methods employed were: sanding, polishing, vacuum furnace heat-treatment and air furnace heat-treatment. Corrosion testing was conducted in supercritical water at 500°C at a pressure of 27 MPa. After 500 h and 940 h exposed to SCW the ground and the polished (to mirror finishing using alumina paste) samples showed little weight gain. Vacuum furnace heat-treatment produced a very light surface film and all samples showed moderate weight gain. However, air furnace heat-treated samples formed surface scales and all samples suffered appreciable weight loss after testing in SCW, except for the Ni20Cr5Al sample. Of the samples tested, Ni20Cr5Al prepared by sanding showed the best performance in terms of weight change when tested at 500°C at a pressure of 27 MPa. This is believed to be associated with higher residual stresses in samples after sanding.

1. Introduction

It has been proposed that a supercritical water-cooled reactor (SCWR) be used as part of the development of next generation (Gen IV) nuclear power generation with the operating conditions outlined in Figure 1 [1,2]. The primary objective is the need to increase the plant efficiency. The supercritical water turbine cycle can reach a thermal efficiency of over 40% compared with an advanced boiling water reactor (BWR) system with 34% maximum efficiency. Also, since the specific volume of supercritical water is small, the size of the main components, such as the turbines, can be made much more compact. Additionally, the recirculation system, steam generators and steam-water separators used in the traditional steam engine plant, can be eliminated due to the absence of a phase change in the supercritical regime [1].

The use of SCW presents challenges to the fluid containment materials due to corrosion concern. Furthermore, material's behaviors in SCW change with fluid properties significantly. Most metal oxides show increased solubility in either acidic or alkaline SCW fluid, so an increase in the ionic character of water will cause an increase in corrosion [3]. The solubility of oxygen is another consideration. Increased oxygen concentration increases the oxidizing power of the fluid. The corrosion rate of different materials is also sensitive to the density of SCW. The corrosion rate has been correlated to the density of the water [4].

Although supercritical water (SCW) has been used as the working fluid in fossil fuel plants [2] and as a high efficiency solvent for organics, a SCW nuclear power plant presents increased

materials challenges due to the effects of radiation on both the alloy and on the coolant; water radiolysis results in the production of oxidizing species which can lead to increased corrosion. , Ferritic-martensitic steels, austenitic stainless steels, and Ni based alloys are some of the candidate materials proposed for an SCWR [5, 6]. However, most of these materials suffer from excessive corrosion at the high temperatures proposed for the CANDU SCWR concept.

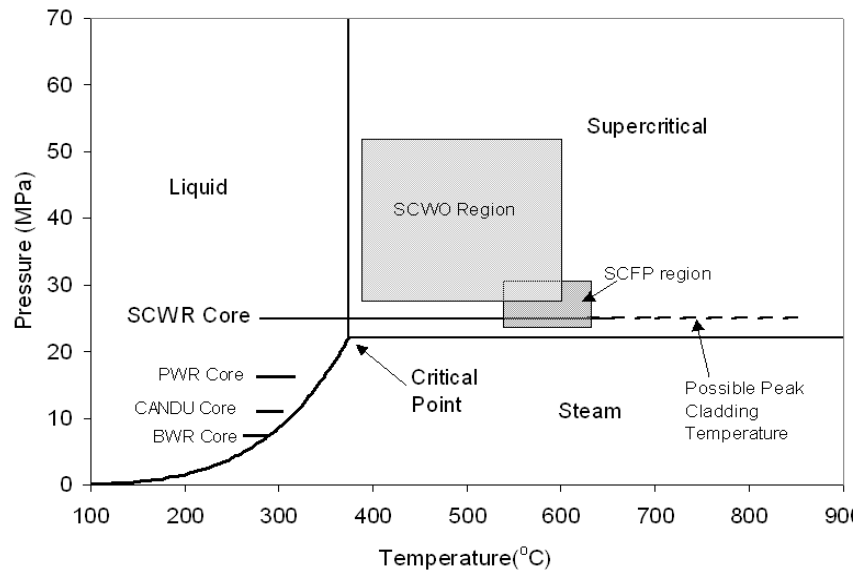


Figure 1 CANDU SCWR operating region [2].

In addition to the impact of fluid properties and material compositions, surface preparation has also shown to influence the corrosion behavior of materials. In a study carried out by Guzonas [7], it was demonstrated that surface finish and temperature were the most important factors on the weight change when 304SS was tested under SCW conditions. The water density and chemistry were found to be less critical. It is therefore the focus of this study to further examine different surface preparation methods. Additionally, four different alloy compositions were tested. These different compositions were designed to independently examine the effect of Cr and Al on the corrosion behavior of Ni based alloy in SCW. The addition of Al was based on the superior corrosion resistance of Al_2O_3 in SCW environment [8, 9].

2. Materials and Experimental Procedure

A total of four 12.7 mm (0.5") diameter rods were created by Sophisticated Alloys INC. These four materials have the compositions Ni20Cr, Ni5Al, Ni50Cr and Ni20Cr5Al. Each rod was cut to a button sample of 3-5 mm in thickness. The samples were cut using a Buehler Isomet 1000 precision saw and then ground to 400 grit on a Buehler Handimet grinder. According to the test design, a second set of samples was ground and polished to a mirror finish using 0.3 μm alumina pastes. A third set of samples was vacuum heat-treated for 24 hours at 1050°C followed by furnace cooling. The fourth set was air heat-treated for 24 hours at 1050°C followed by air cooling. **Error! Reference source not found.** Table 1 summarizes the surface processing details for each set of samples. Each set included samples with four different compositions. All samples were cleaned with alkaline solution in a Branson 2520 ultrasonic cleaner followed by methanol

rinse and air drying.

Table 1 Surface preparation methods.

Sample set	Ground with 400 grit sand paper (G)	Polished to mirror finishing (P)	Vacuum heat treatment (VHT)	Air heat treatment (AHT)
1	√			
2	√	√		
3	√	√	√	
4	√	√		√

Tests were carried out in an autoclave (Parr 4650 combined with a Parr 4838 reactor controller). The samples were hung on the alumina arms (McMaster Carr, USA) of a customized 316 stainless steel tree which was placed on a ceramic disc in the vessel in order to prevent contact with the vessel itself. Also, alumina spacers were placed between the specimens to prevent the samples from contacting each other. A vacuum was created in the vessel and a calculated amount of water was injected into the vessel to give the proper pressure at the test temperature. The dissolved oxygen concentration in the water was controlled by distillation and nitrogen gas bubbling. The final dissolved oxygen content was measured before each test run. After test completion, a water sample was taken. The pH was measured and compared to that before the test; a slight decrease in pH was observed after testing. **Error! Reference source not found.** Table 2 provides a summary of the test conditions.

Table 2 Test Parameters.

Test Stage	Temp (°C)	Pressure (start/end) (MPa)	Time (hrs)	DO level (ppm)	pH value (start/end)	Density (start/end) (Kg/m ³)
Stage 1	500	27.58/25.92	500	1.0	6/5	102.4/94.17
Stage 2	495-540	27.58/22.41	440	0.6	6/5	104.2/70.45

Due to the leakage of the autoclave, the pressure decreased slightly during stage 1. For stage 2, it decreased somewhat faster. Conditions were kept within the supercritical region by raising the temperature from 495 to 540°C. The plots of temperature and pressure as a function of the time are shown in Figure 2.

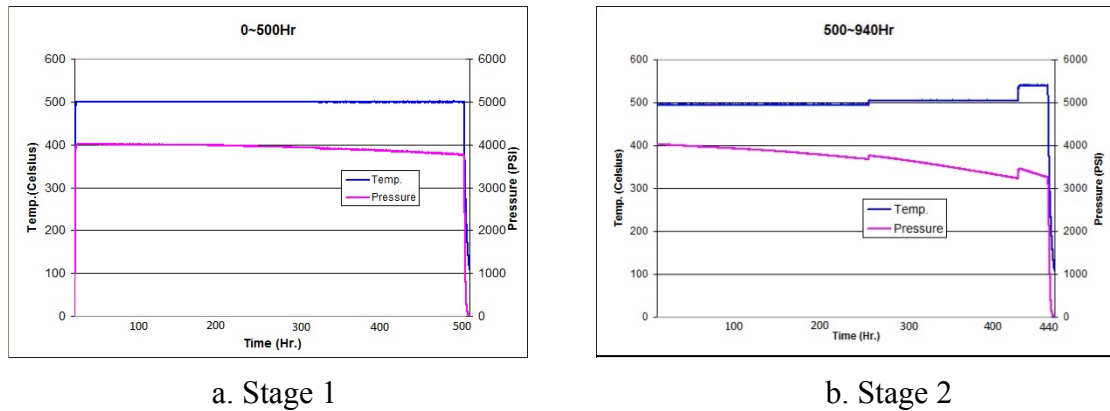


Figure 2 Pressure versus time for stage 1 (a) and stage 2 (b) of the test

3. Results and Discussion

3.1 Visual observation

Upon removing the samples from the autoclave after each stage of the testing, their surface appearances were recorded as shown in Figure 3. The surface scales varied with composition and surface preparation. Samples without any heat treatment (P and G) appeared quite smooth and some displayed metallic shine. The vacuum heat-treated samples exhibited darker surface features than the polished and ground samples. Several air furnace heat-treated samples (Ni20Cr and Ni5Al) showed heavy scale and scale spalling. The surface condition did not change significantly after 940 h testing compared with that after 500 h test.

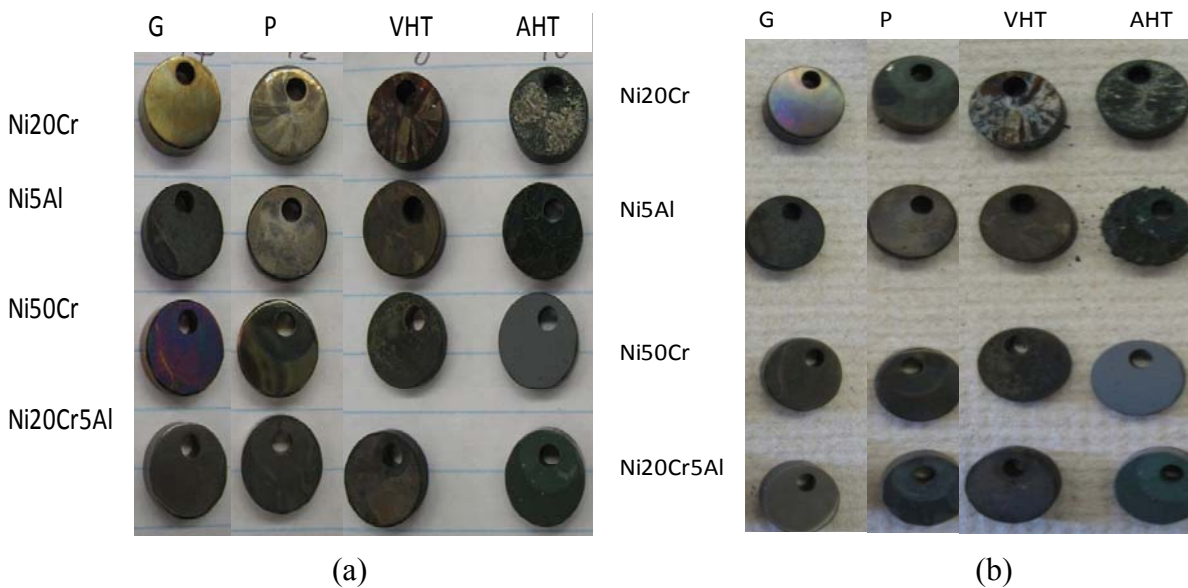


Figure 3 Sample surface conditions after 500 h (a) and 940 h (b) test.

3.2 Sample weight changes

Sample weights right before and after testing are shown in Figure 4, representing the results after

the first 500 h, after the next 440 h, and finally the cumulative 940 h. Overall, the samples that had been ground and polished showed the least weight gain, while the air heat-treated samples showed a significant weight loss after 500 h exposure to SCW. Scale spalling was believed to be the cause for the weight loss in some of the air heat treated samples (Ni20Cr and Ni50Cr). Small blackish particles were found in the water after each stage of the test. Vacuum heat treatment seemed to have caused more weight gain during the first 500-hour exposure to SCW than the stage 2 of the test. Ni20Cr5Al exhibited the lowest and most consistent weight change compared to the other samples. This was also the only air heat-treated sample that did not experience weight loss.

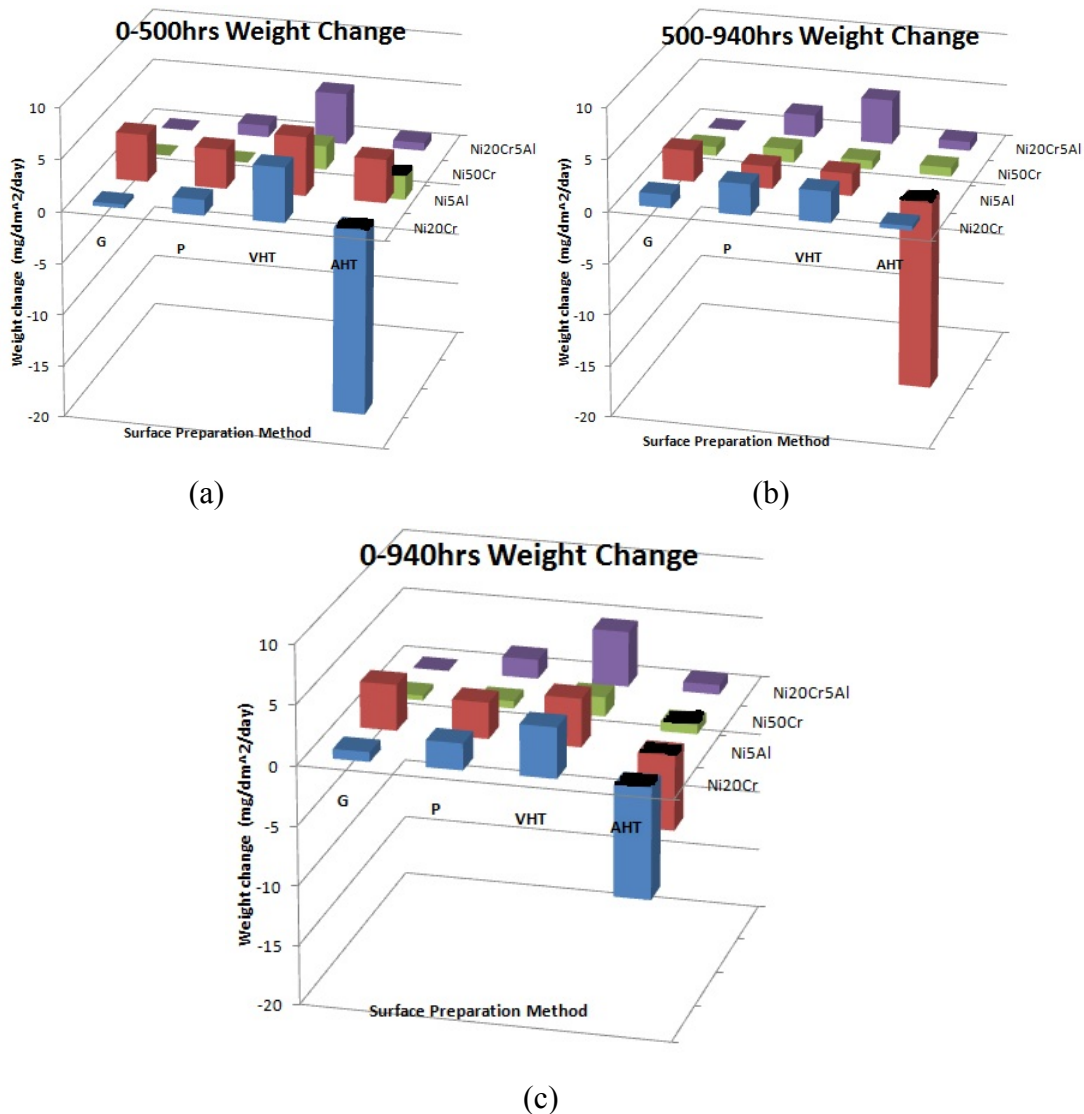


Figure 4 3-D bar chart showing the weight change (Z-axis) as a function of surface preparation (X-axis) and sample type (Y-axis) after the first 500 h (a), next 440 h (b) and the cumulative weight change (c).

During the stage 2 of the test, the weight changes seemed to have stabilized and all samples displayed a slight weight gain (except for the air heat-treated Ni5Al sample, which experienced scale spalling in the stage 2). Samples that have been ground with 400 grit sand paper showed the least weight change.

The cumulative weight change after 940 h exposure to SCW showed a similar trend to that observed after the first 500 h, i.e., grinding and polishing resulted in lower and stable weight gain for all sample compositions while air furnace heat-treatment caused weight loss to samples Ni20Cr, Ni5Al and Ni50Cr due to spalling of the surface scale. Vacuum furnace heat-treatment resulted in steady surface film formation for all sample compositions. The surface morphology of various samples is further discussed in the next section.

3.3 SEM surface analysis

3.3.1 Samples before SCW test

The surface morphology was characterized using SEM along with chemical composition analysis. The vacuum and air heat-treated samples were analyzed before exposure to SCW, and all 4 sets of samples were examined after the 940 h test. The heat treatments prior to SCW exposure were intended to promote the formation of a thin oxide film. The type of the oxide formed depends upon the sample composition. The EDS results showed that alumina was formed on vacuum heat-treated Ni20Cr5Al, (**Error! Reference source not found.**) while chromia formation was observed on the air heat-treated Ni20Cr and Ni50Cr samples. The EDS analysis results from heat treated surface are summarized in **Error! Reference source not found.**

Table 3 EDS surface analysis results for samples after VHT and AHT (wt%).
 (*: oxygen eliminated mathematically)

		Al	Cr	Ni	O
Ni20Cr	Nominal composition	-	20	80	-
	Vacuum H/T	-	16.9	83.1	-
		-	16.9	83.1	*
	Air Furnace H/T	-	14.95	58.95	26.1
-		20.23	79.77	*	
Ni5Al	Nominal composition	5	-	95	-
	Vacuum H/T	4.52	2.71	92.77	-
		4.52	2.71	92.77	*
	Air Furnace H/T	5.88	-	85.3	8.82
6.45		-	93.55	*	
Ni50Cr	Nominal composition	-	50	50	-
	Vacuum H/T	-	37	60.56	2.44
		-	37.93	62.07	*
	Air Furnace H/T	-	63.78	-	36.22
-		100	-	*	
Ni20Cr5Al	Nominal composition	5	20	75	-
	Vacuum H/T	11.27	6.55	76.88	5.29
		11.9	6.92	81.18	*
	Air Furnace H/T	8.84	29.39	42.26	19.51
10.98		36.51	52.51	*	

The sample surface morphologies after vacuum heat treatment are shown in Figure 5. While the Ni20Cr and Ni5Al samples exhibited very smooth and light surface features, the oxides formed on samples of Ni50Cr and Ni20Cr5Al are quite porous.

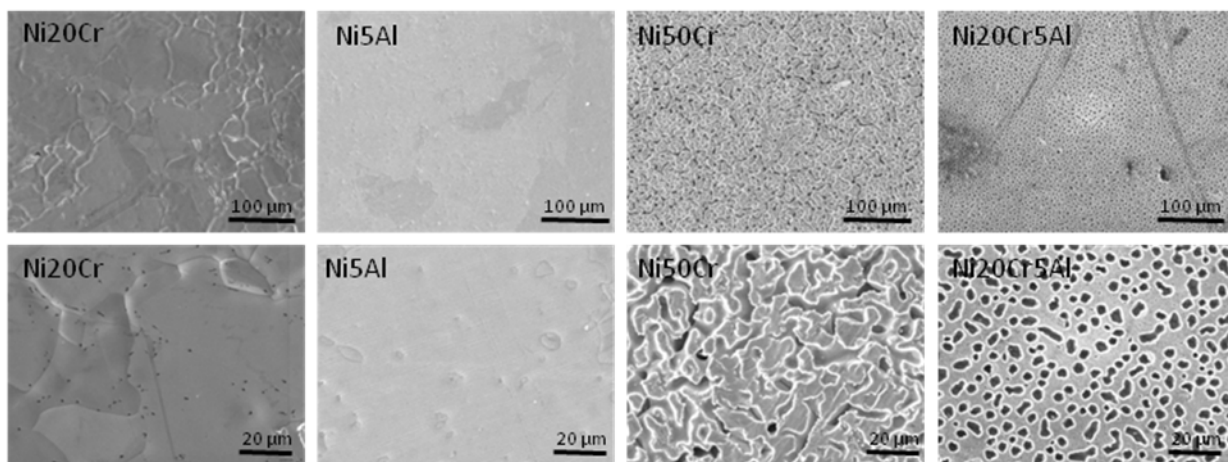


Figure 5 SEM images (top: low mag., bottom: high mag.) of four samples in the as-heat treated condition before testing (vacuum).

The air furnace heat-treated samples had different surface morphologies than the vacuum heat-treated samples. The Ni20Cr sample was covered with a thick oxide layer (**Figure 6**) with angular morphology, suggesting more oxide growth under this condition. The Ni5Al sample showed no evidence of a surface oxide, and some localized surface pitting was observed. Surface scale flaking was observed for the Ni50Cr and Ni20Cr10Al samples, although oxide films formed under the scale. The surface compositions after air furnace heat-treatment are summarized in **Error! Reference source not found.**

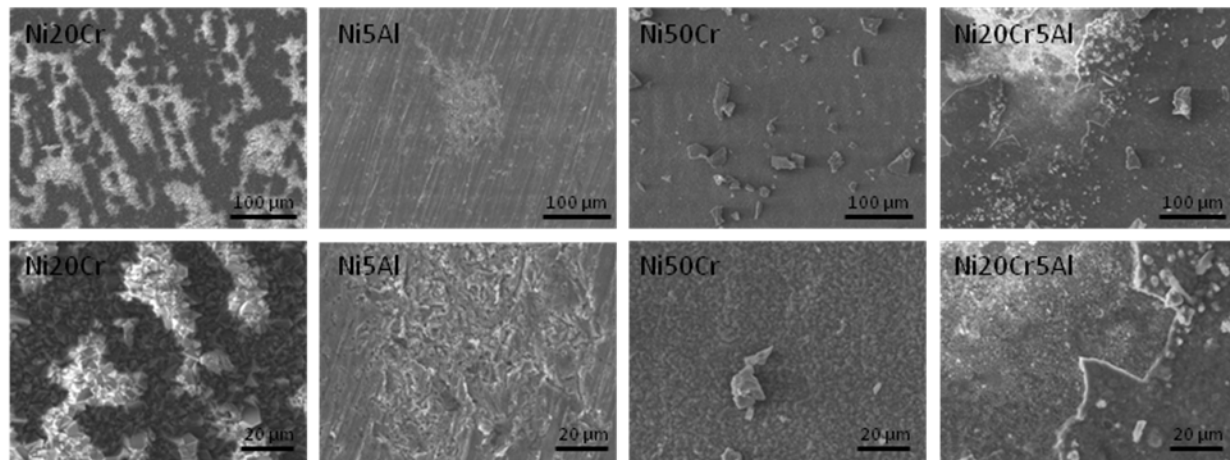


Figure 6 SEM images of samples in the as heat-treated condition.

3.3.2 Samples after SCW exposure

The surface features of the Ni20Cr sample showed that both ground and polished surfaces still maintained the original surface preparation features, i.e., polishing lines. The images also showed the deposition of spherical Si-rich contaminants (from the use of silicon sealant in the system). The Cr content was higher than the nominal composition in the ground sample (**Error! Reference source not found.**) suggesting possible Cr diffusion to the surface due to cold working. The vacuum heat-treated sample continued to develop a surface film within the grains and along the grain boundaries, while the air heat-treated sample displayed surface scale delamination. The surface film formed on vacuum heat-treated samples after SCW exposure is believed to contain Cr-rich and Ni-rich oxides based on the chemical composition given in **Error! Reference source not found.**, as no enrichment of Cr was detected. Cr depletion was found on the air heat-treated sample, and spallation of the Cr-rich oxide may have occurred this sample. Since all samples were found to have been contaminated by a Si-rich material, Si was excluded from the EDS analysis in order to properly quantify the concentrations of oxygen and metallic elements. The findings from the SEM analysis were consistent with the weight change results given in Figure 5, where the air heat-treated Ni20Cr showed a weight loss, while the polished and ground samples exhibited small weight gains.

Table 4 EDS surface analysis results for the Ni20Cr sample after 940 h SCW exposure (wt%).

Ni20Cr	Cr	Ni	O
Ground	25.57	53.44	20.99
	32.36	67.64	*
Polished	7.93	52.69	39.38
	13.08	86.92	*
Vacuum H/T	18.05	67.9	14.05
	21	79	*
Air Furnace H/T	6.01	68.39	25.6
	8.08	91.92	*

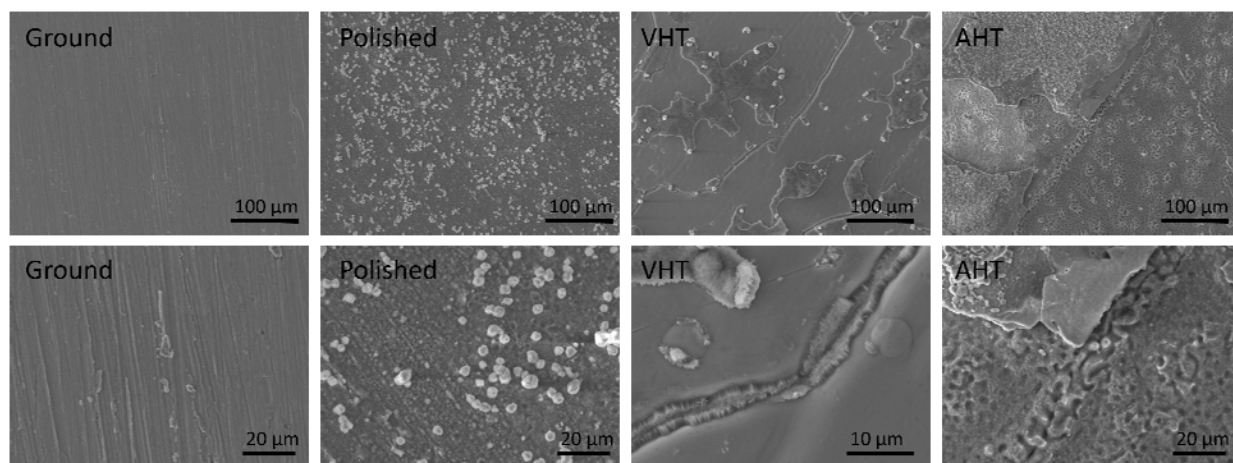


Figure 7 SEM images of Ni20Cr samples after 940 h SCW exposure.

The surface preparation methods also significantly influenced the surface morphology of the Ni5Al samples. Grinding and polishing resulted in comparable surface features (scratch lines) after testing while vacuum heat-treatment revealed island-like phase formation. In particular, air furnace heat-treatment generated heavy surface scale which began to delaminate upon exposure to SCW, causing weight loss. EDS analysis results (**Error! Reference source not found.**) confirmed oxide formation on the surface. The Al content was slightly elevated for the air heat-treated sample, suggesting more alumina formation as a result of heat treatment. Other samples showed similar Al and Ni contents as the nominal composition when oxygen was excluded.

Table 5 EDS analysis results of surface compositions for the Ni5Al sample after 940 h exposure to SCW (wt%).

Ni5Al	Al	Ni	O
Ground	4.14	69.33	26.53
	5.63	94.37	*
Polished	3.05	73.86	23.09
	3.97	96.03	*
Vacuum H/T	3.57	79.71	16.72
	4.29	95.71	*
Air Furnace H/T	5.32	57.2	37.48
	8.51	91.49	*

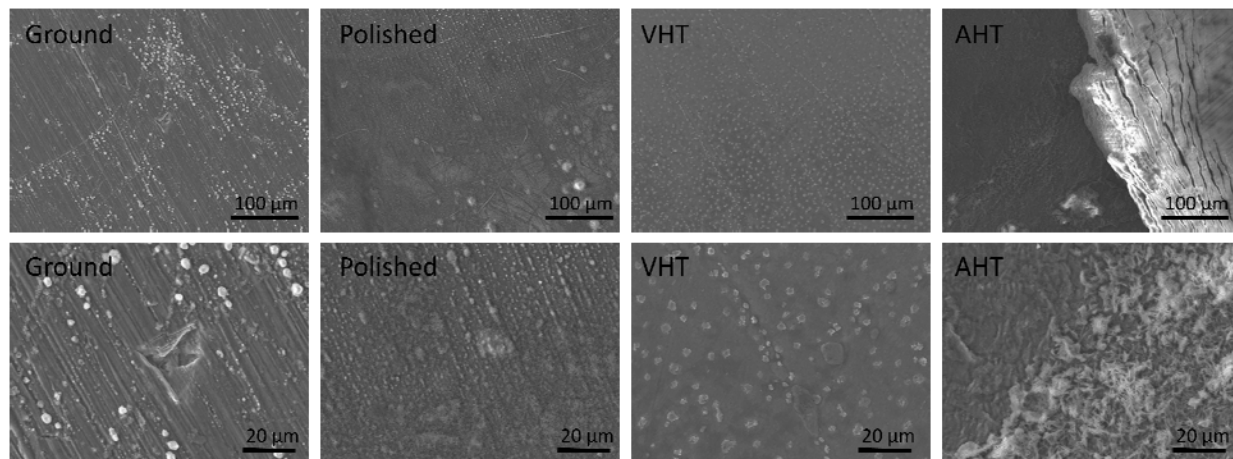


Figure 8 SEM images of Ni5Al samples after 940 hr exposure to SCW at 500°C, 27 MPa.

For the Ni50Cr samples, the surface morphology changed somewhat from that of Ni20Cr, as shown in Figure 9. The ground surface was largely intact with visible scratch lines from grinding, while small surface depressions were observed on the polished surface. Elevated Cr content compared to the nominal composition was detected on the ground surface after 940 h SCW testing. The vacuum heat-treated sample showed the formation of a porous surface phase, and from the EDS results, given in Table 6, it is likely to be Ni-rich oxide (NiO). The most noticeable changes were the complete lack of scale loss in the as-heat-treated Ni50Cr sample (Figure 6) and the presence of a discrete phase on the surface. Since Ni was not detected on the surface (**Error! Reference source not found.**), these discrete particles are believed to be Cr₂O₃. The weight loss for the air heat-treated Ni50Cr sample was moderate, indicating the more adherent nature of the chromium oxide formed compared to the film that formed on the low Cr sample (Ni20Cr).

Table 6 EDS surface analysis results for sample Ni50Cr after 940 h exposure to SCW at 500°C and 27 MPa (wt%).

Ni50Cr	Cr	Ni	O
Ground	43.42	28.32	28.26
	60.52	39.48	*
Polished	43.07	40.37	16.56
	51.62	48.38	*
Vacuum H/T	19.42	45.65	34.93
	29.84	70.16	*
Air Furnace H/T	63.63	-	36.37
	100	-	*

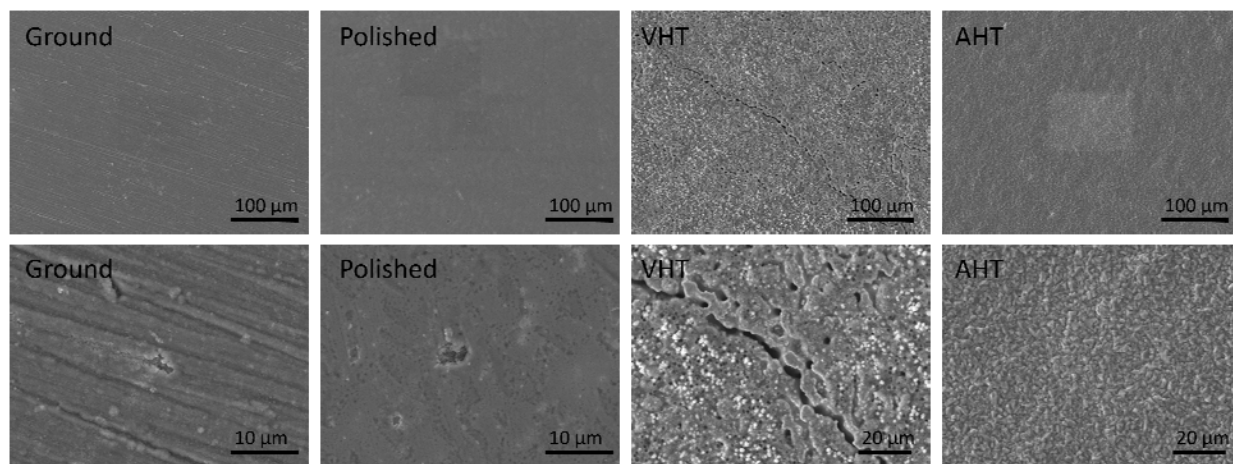


Figure 9 SEM images of Ni50Cr samples after 940-hr exposure to SCW at 500°C and 27 MPa.

The Ni20Cr5Al samples exhibited the best corrosion resistance of the four alloys tested. The ground sample showed very little difference compared to the sample before SCW testing; only polishing lines are visible, as shown in Figure 10. The EDS results (**Error! Reference source not found.**) also confirmed minimal changes in the surface composition. It is apparent that this alloy would be a good choice for further testing for use in a SCW reactor. The polished sample showed a slightly uneven surface after SCW testing, however, no obvious pitting was observed. For vacuum and air furnace heat-treated samples, the samples seemed to have formed a protected layer enriched in Al and Cr/Al, respectively. Since vacuum heat treatment is known to promote Al₂O₃ formation, it is believed that a thin Al₂O₃ layer formed on the surface prior to the SCW test. Air furnace heat treatment encouraged both Cr₂O₃ and Al₂O₂ formation as shown by the elevated Cr and Al content on the surface (**Error! Reference source not found.**).

Table 7 EDS analysis results of surface compositions for sample Ni20Cr5Al after 940 h exposure to SCW at 500°C and 27 MPa (wt%).

Ni20Cr5Al	Cr	Al	Ni	O
Ground	19.35	3.83	68.15	8.67
	21.19	4.19	74.62	*
Polished	8.84	1.22	51.85	38.09
	14.28	1.97	83.75	*
Vacuum H/T	3.23	6.44	68.18	22.15
	4.15	8.27	87.58	*
Air Furnace H/T	28.63	5.36	36.18	29.83
	40.8	7.64	51.56	*

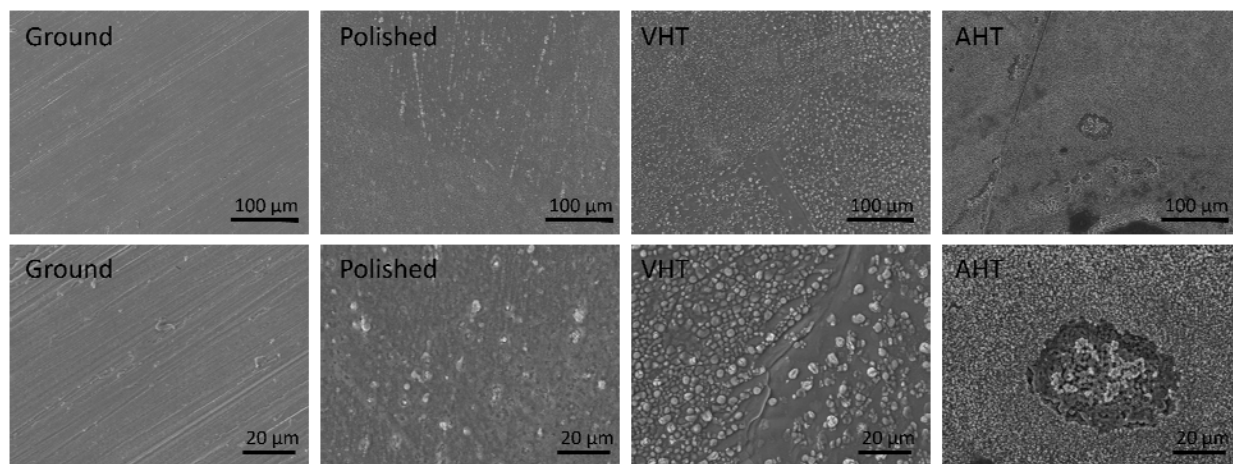


Figure 10 SEM images of Ni20Cr5Al samples after 940-hr exposure to SCW at 500°C and 27 MPa.

4. Conclusion

The effect of surface preparation methods on the corrosion behavior of four Ni-based alloys was examined. Test samples with various compositions (Ni20Cr, Ni5Al, Ni50Cr, and Ni20Cr5Al) were prepared using sanding, polishing, vacuum and air furnace heat-treatment. Corrosion testing was conducted in supercritical water at 500°C at a pressure of 27 MPa. After 500 and 940 h exposures to SCW, samples with surfaces prepared with 400 grit sandpaper grinding and polishing (to a mirror finishing) showed very little weight gain, and their surface morphology was not affected appreciably by the SCW exposure. Vacuum furnace heat-treatment produced a very light surface film and all samples showed moderate weight gain after testing. However, samples that were air furnace heat-treated formed surface scales and all samples except Ni20Cr5Al suffered weight loss. This weight loss was due to the spalling of the oxides formed

during heat treatment during exposure to SCW. Of all the samples tested, Ni20Cr5Al prepared with 400 grit sandpaper showed the best performance with respect to weight change under the test conditions.

5. Acknowledgement

The authors would like to thank NSERC and AECL for providing a CRD grant to support this work.

6. References

- [1] Junya Kaneda, Shigeki Kasahara, Jiro Kuniya, Kumiaki Moriya, Fumihisa Kano, Norihisa Saito, Akio Shioiri, Tamaki Shibayama and Heishichiro Takahashi, "General corrosion properties of titanium based alloys for the fuel claddings in the Supercritical Water-Cooled Reactor", Proceedings of the 12th International Conference on Environmental Degradation of Materials in Nuclear Power System-Water Reactors, TMS, 2005.
- [2] D. Guzonas, "SCWR materials and chemistry status of ongoing research", GIF Symposium, Paris, France, Sept. 9-10, 2009.
- [3] Peter Kritzer, "Corrosion in high-temperature and supercritical water and aqueous solutions: a review", *Journal of Supercritical Fluids*, Vol.29, 2004, pp.1-29.
- [4] Tulkki, V. "Supercritical Water Reactors", Master's Thesis, Helsinki University of Technology, November 2006.
- [5] Seong Sik Hwang, Byung Hak Lee, Jung Gu Kim and Jinsung Jang, "SCC and Corrosion evaluations of the F/M steels for a supercritical water reactor", *Journal of Nuclear Materials*, Vol.372, Iss.2-3, 2008, pp. 177-181.
- [6] Q. J. Peng, S. Teyseyre, P. L. Andresen and G. S. Was, "Stress corrosion crack growth in type 316 stainless steel in supercritical water", *Corrosion*, Vol. 63 (11), 2007, pp.1033-1041.
- [7] D.Guzonas, J.Wills, H.Dole, J.Michel, S.Jang, M.Haycock and M.Chutumstid, "Steel corrosion in supercritical water: an assessment of the key parameters", the 2nd Canada-China Joint Workshop on Supercritical Water-Cooled Reactors (CCSC-2010), Toronto, ON, Canada, April 2010.
- [8] Kohei Oda and Tetsuo Yoshi, "Hydrothermal corrosion of alumina ceramics", *J. Am. Ceram. Soc.* 80 (12), 1997, pp.3233-36.
- [9] Nikolaos Boukis, Nils Claussen, Klaus Ebert, Rolf Janssen and Michael Schacht, "Corrosion screening tests of high-performance ceramics in supercritical water containing oxygen and hydrochloric acid", *Journal of the European Ceramics Society*, 17, 1997, pp.71-76.